doi:10.1016/j.jmb.2005.01.017 J. Mol. Biol. (2005) 347, 465–477

JMB

Available online at www.sciencedirect.com

SCIENCE DIRECT®

ELSEVIER

Solution Structures of the Core Light-harvesting α and β Polypeptides from *Rhodospirillum rubrum*: Implications for the Pigment–Protein and Protein–Protein Interactions

Zheng-Yu Wang*, Kazutaka Gokan, Masayuki Kobayashi and Tsunenori Nozawa

Department of Biomolecular Engineering, Graduate School of Engineering, Tohoku University Aramaki-aza, Aoba, Aoba-ku Sendai 980-8579, Japan

**Corresponding author*

We have determined the solution structures of the core light-harvesting (LH1) α and β-polypeptides from wild-type purple photosynthetic bacterium *Rhodospirillum rubrum* using multidimensional NMR spectroscopy. The two polypeptides form stable α helices in organic solution. The structure of α-polypeptide consists of a long helix of 32 amino acid residues over the central transmembrane domain and a short helical segment at the N terminus that is followed by a three-residue loop. Pigment-coordinating histidine residue (His29) in the α-polypeptide is located near the middle of the central helix. The structure of β-polypeptide shows a single helix of 32 amino acid residues in the membrane-spanning region with the pigment-coordinating histidine residue (His38) at a position close to the C-terminal end of the helix. Strong hydrogen bonds have been identified for the backbone amide protons over the central helical regions, indicating a rigid property of the two polypeptides. The overall structures of the *R. rubrum* LH1 α and β-polypeptides are different from those previously reported for the LH1 β-polypeptide of *Rhodobacter sphaeroides*, but are very similar to the structures of the corresponding LH2 α and β-polypeptides determined by X-ray crystallography. A model constructed for the structural subunit (B820) of LH1 complex using the solution structures reveals several important features on the interactions between the LH1 α and β-polypeptides. The significance of the N-terminal regions of the two polypeptides for stabilizing both B820 and LH1 complexes, as clarified by many experiments, may be attributed to the interactions between the short N-terminal helix (Trp2-Gln6) of α-polypeptide and a GxxxG motif in the β-polypeptide.

Keywords: membrane protein; pigment binding; photosynthesis; transmembrane helix; GxxxG motif

Introduction

The bacterial photosynthetic apparatus provides a simplified model system ideally for studying the light energy conversion, pigment–membrane protein interaction, and assembly of multicomponent complexes. In purple photosynthetic bacteria, the light energy is absorbed by two types of light-harvesting complexes (LH1, LH2), and then is transferred rapidly and efficiently to the reaction center (RC) where the primary charge separation takes place across the membrane and a cyclic electron transport chain is formed. The LH1 complex is located intimately around the RC with a fixed stoichiometric ratio, whereas the LH2 complex is arranged in the periphery of the RC–LH1 complex with varied ratios to the RC

Abbreviations used: BChl, bacteriochlorophyll; LH1, core light-harvesting; LH2, peripheral light-harvesting; B820 and B777, core light-harvesting complex subunits absorbing at 820 nm and 777 nm; HPLC, high-performance liquid chromatography; OG, *n*-octyl β-D-glucopyranoside; SANS, small-angle neutron scattering.

E-mail address of the corresponding author: wang@biophys.che.tohoku.ac.jp

depending on growth conditions such as light intensity and temperature. Both LH1 and LH2 are large oligomers of a basic structural unit composed of a heterodimer of two small integral membrane polypeptides (α and β, ca 6 kDa) associated with bacteriochlorophyll (BChl) and carotenoid molecules. Among these complexes, there have been a number of high-resolution structures available for the RC[1,2] and LH2,[3,4] which have greatly enhanced our understanding of the mechanism of photosynthesis and pigment-membrane protein assembly. However, such structural information has been lacking for the LH1 complex due to difficulties in isolating a stable intact complex and preparing high-quality crystals. Two-dimensional projection maps at 8.5 Å resolution have been produced by electron microscopy for both reconstituted and native RC–LH1 complexes from *Rhodospirillum rubrum*.[5,6] These maps showed a closed ring composed of 16 LH1 αβ pairs around the RC. Similar structure was also observed by atomic force microscopy for the RC–LH1 complex in the native photosynthetic membrane of *Rhodopseudomonas viridis*[7] and on two-dimensional crystals from *R. rubrum*.[8] A different structural arrangement was reported for the RC–LH1 complex of *Rhodobacter sphaeroides* based on the observations made by electron cryomicroscopy and atomic force microscopy.[9,10] The two-dimensional projection map at about 20 Å resolution revealed an S-shaped oligomeric structure of the LH1 αβ subunit around the RC with two gaps in the oligomer lacking protein density. Recently, the resolution has been improved to 4.8 Å for an RC–LH1 complex from *Rhodopseudomonas palustris*.[11] It shows that the RC is surrounded by an oval LH1 complex consisting of 15 pairs of the αβ polypeptides, and the repeating αβ units appear to be interrupted by an unknown protein W.

Apart from crystal structure determination of the whole LH1 or RC–LH1 complexes, efforts have also been made to elucidate the structure of the basic unit and its individual components. Upon addition of detergents, the LH1 multimer can be dissociated into a stable structural subunit characterized by the Q_y absorption band at 820 nm.[12] Both the subunit (referred to as B820) and LH1 complex can be reversibly dissociated and reconstituted from their components.[13] The B820 subunit has been shown by many biochemical and spectroscopic studies to consist of one pair of αβ polypeptides and two BChl *a* molecules;[14–19] its structure–function relationship has been extensively investigated by reconstitution using various modified polypeptides and pigment molecules.[20–25] Although no atomic-level structure is yet available for the B820 subunit, the two BChl *a* molecules within the subunit have been shown to have non-equivalent conformation, where the acetyl and keto carbonyl groups form strong hydrogen bonds with the polypeptides.[17,26,27] Determination of the structure of individual LH1 polypeptides has been done by solution NMR for the β-polypeptide of *Rb. sphaeroides*.[28–30] Essentially the same structure, characterized by a bent conformation with two short α-helical portions joined by a flexible central hinge, has been obtained in both organic solvents and detergent solution. So far, the structure of the LH1 α-polypeptide has not been reported.

We have determined the solution structures of native LH1 α and β-polypeptides from *R. rubrum* using multidimensional NMR spectroscopy. High-resolution structures are obtained in mixed organic solvents using ^{13}C and ^{15}N-labeled samples In contrast to those reported for the β-polypeptide of *Rb. sphaeroides*, both the polypeptides of this study exhibit a long α-helical region over the central transmembrane domain. Strong hydrogen bonds are identified for all of the backbone amide protons in the helical region of the two polypeptides. The overall structural feature is very similar to that of the corresponding LH2 α and β-polypeptides determined by X-ray crystallography.

Results

Secondary structures as determined by CD spectra

To ensure that both the α and β-apopolypeptides maintain their secondary structures in organic solvent, we measured the CD spectra by dissolving the samples in acetonitrile/2-propanol (2:1) containing 0.1% trifluoroacetic acid (TFA), which was used as elution buffer at the final step of purification. Figure 1 shows the results. As expected from the hydrophobicity analysis and the common nature of integral membrane proteins, both the polypeptides exhibited similar spectral shapes with strong characteristics of helical structure. The calculated α-helical contents were 71% and 57% for the α and β-apopolypeptides, respectively. The result is consistent with that of LH1 β-polypeptide from

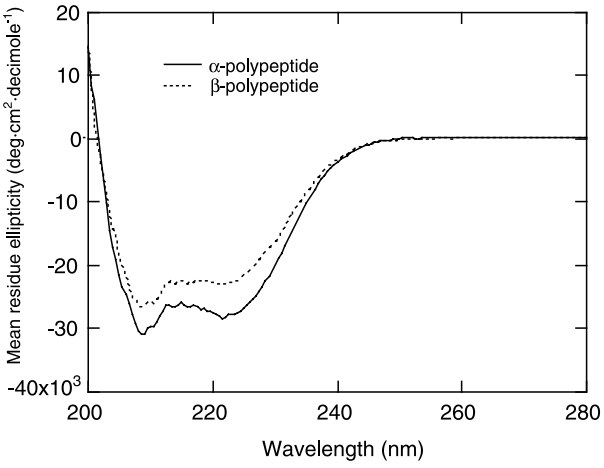

Figure 1. CD spectra of the *R. rubrum* LH1 α-polypeptide (continuous curve) and β-polypeptide (dotted curve) in 2:1 (v/v) acetonitrile/2-propanol containing 0.1% (v/v) TFA.

Rb. sphaeroides in organic and detergent solutions,[28] and those of LH2 polypeptides calculated from X-ray crystal structures.[3,4] The latter also showed that LH2 α-apopolypeptide had higher helical content than LH2 β-apopolypeptide. The CD result provides evidence that overall structures of the LH1 polypeptides of this study are well retained in the mixed organic solvents.

Resonance assignments of NMR spectra

Although the LH1 α-apopolypeptide of *R. rubrum* consists of only 52 amino acid residues, there are ten Leu residues and most of them are located in the central hydrophobic domain. The highly uneven distribution in the amino acid residues resulted in heavy degeneracy of the NMR signals. As a consequence, the ^{1}H–^{15}N correlation spectrum of uniformly ^{15}N-labeled α-polypeptide exhibited a very limited chemical shift dispersion characteristic of helical proteins (Figure 2(a)). Due to the overlap of amide resonances for the ^{13}C and ^{15}N-labeled samples, backbone sequential assignment could not be made by any single triple-resonance experiment. CBCANH and CBCA(CO)NH proved to be the most efficient set of experiments for the sequential

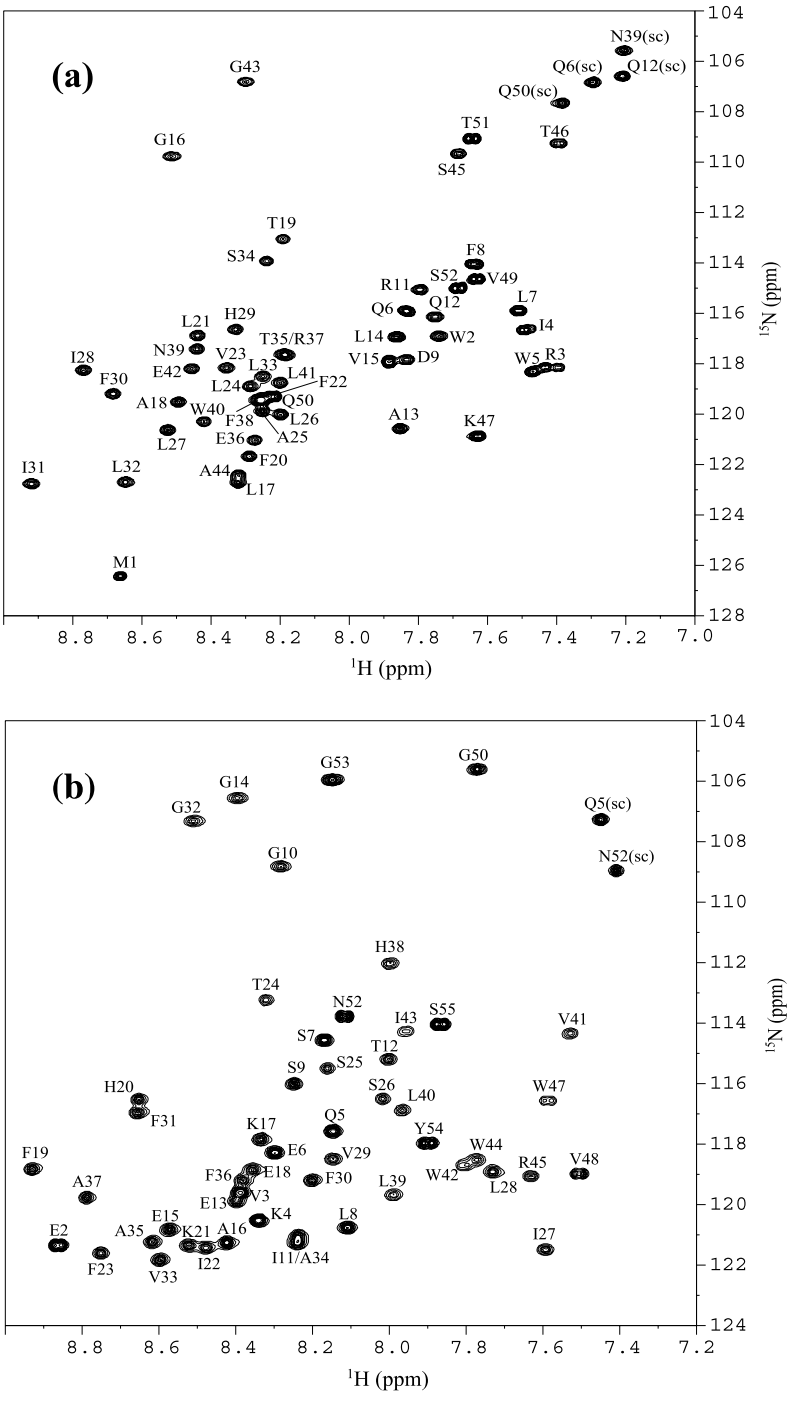

Figure 2. ^{1}H–^{15}N HSQC spectra of the *R. rubrum* LH1 (a) α-polypeptide and (b) β-polypeptide. The spectra were recorded using 1 mM ^{15}N-labeled polypeptides in $CDCl_3/CD_3OH$ (1:1, v/v) at 25 °C. Backbone amide cross-peaks are labeled according to residue type and sequence number. The peaks with an additional label of (sc) correspond to Gln and Asn side-chain NH_2 groups.

assignments, which correlate the C^{α} and C^{β} resonances of the preceding residue with intraresidue backbone ^{15}N, H^N, C^{α} and C^{β} resonances. A sample series of correlated intraresidue and interresidue C^{α}/C^{β} resonances is shown in Figure 3(a) for the residues around His29 of α-polypeptide. With a large number of experiments, complete backbone resonances (H^N, N, C^{α} and CO) were assigned for the α-polypeptide, and the results are indicated in Figure 2(a). Most N and C-terminal amide protons gave resonances in a chemical shift range of δ_H= 7.4–7.9 ppm, while almost all amide protons of the central hydrophobic domain had chemical shifts in a range of δ_H=8.1–8.9 ppm. The strongest signals and best resolution were observed for the residues at both ends of the α-polypeptide. Side-chain assignments were made mainly by ^{15}N total correlated spectroscopy (TOCSY)-heteronuclear single quantum coherence (HSQC) and H(CC)(CO)NH, as HCCH-TOCSY only gave limited numbers of resolved resonances due to the degeneracy in the ^1H–^{13}C correlation spectra.

In contrast to the α-polypeptide, assignment for the β-polypeptide was relatively straightforward. Figure 2(b) shows the 2D ^1H–^{15}N HSQC spectrum of β-polypeptide along with the assignment for the amide resonances. Backbone sequential assignments can be made by a sole HNCA experiment, which correlates the C^{α} resonances of the preceding residue with intraresidue backbone ^{15}N, H^N and C^{α} resonances. A typical example is shown in Figure 3(b) for the sequence from Phe36 to Leu40. Similar to the α-polypeptide, the backbone amides at the N and C-terminal ends of the β-polypeptide exhibited the strongest resonances in the NH region, as can be confirmed from the HSQC spectrum (Figure 2(b)). All resonances from side-chain NH_2 groups of Asn and Gln residues together with those of the indole NH groups of Trp residues were identified. Side-chain assignments were made using ^{15}N TOCSY-HSQC combined with 3D CBCANH and HBHANH spectra; the latter correlates the H^{α} and H^{β} resonances of the preceding residue with intraresidue backbone ^{15}N, H^N, H^{α} and H^{β} resonances. An attempt to correlate side-chain resonances with the assigned H^{α} resonances by a 2D TOCSY spectrum using unlabeled β-polypeptide in $C^2HCl_3/C^2H_3O^2H$ (1:1) at several mixing times had only limited success, owing to severe overlap of the aliphatic proton resonances.

Structure determinations

A total of 400 and 456 unambiguous NOE-derived distance restraints were obtained from 3D ^{15}N NOESY-HSQC experiments for the α and β-polypeptides, respectively. Figure 4 summarizes the details of the amide NOE patterns. Strong NOEs were confirmed for the $H^N(i)$ and $H^N(i+1)$ pairs over extensive ranges of amino acid residues of both the polypeptides, which is considered as a characteristic of an α-helix. Average numbers of the NOE restraints per residue were 16.8 and 19.2 for the residues in the central regions from Gln12 to Glu36 of α-polypeptide and from Glu15 to Ile43 of β-polypeptide, respectively. We have identified a total of 36 and 39 hydrogen bonds for the amide protons of the α and β-polypeptides, respectively,

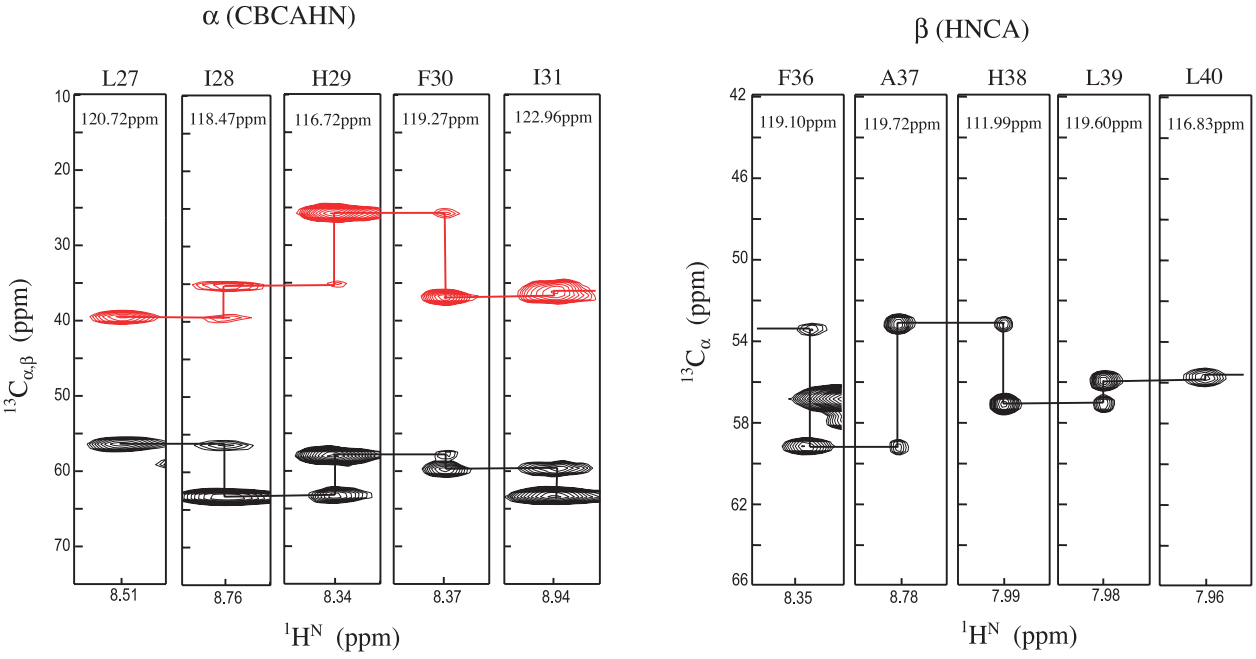

Figure 3. Selected strips of sequential connectivities for the residues around the putative BChl *a*-binding histidine residues. (a) 3D CBCANH strips of Leu27-Ile31 for the LH1 α-polypeptide. Positive (C^{α}) and negative (C^{β}) contours are drawn in black and red, respectively. (b) 3D HNCA strips of Phe36-Leu40 for the LH1 β-polypeptide. The ^{15}N chemical shift is shown in each panel.

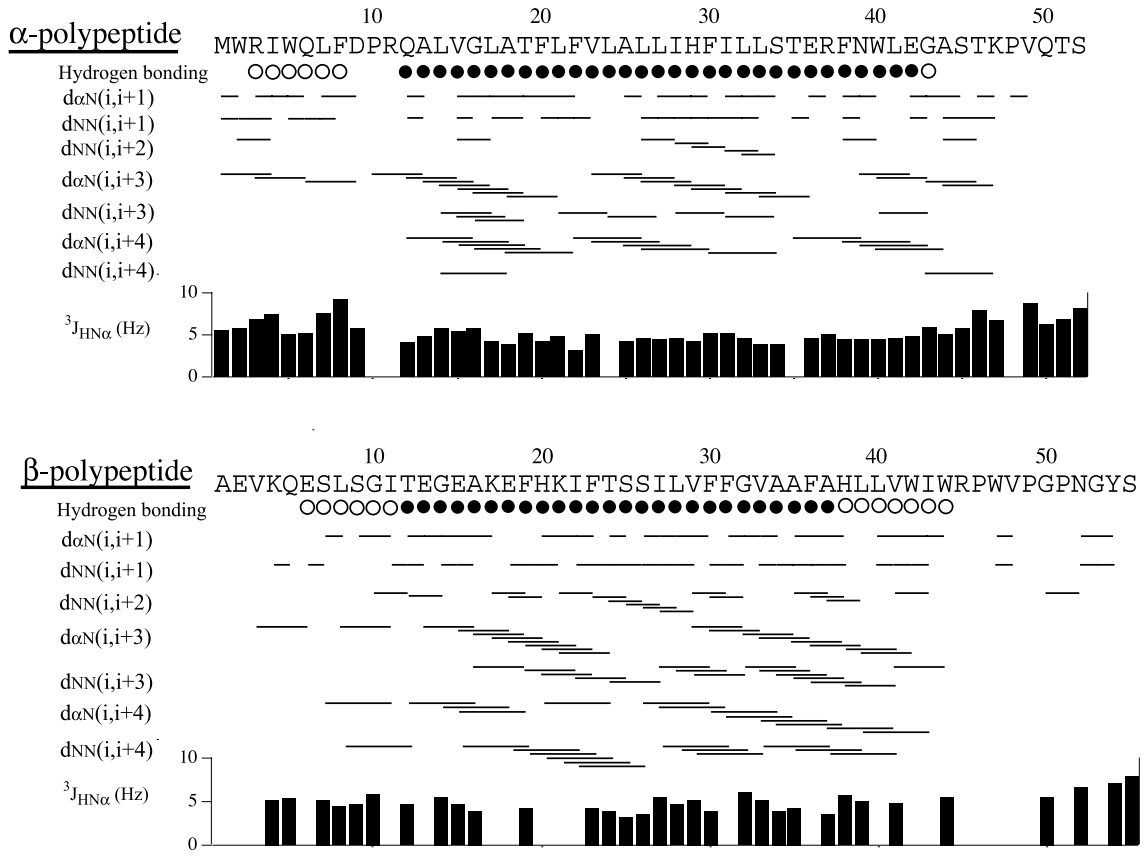

Figure 4. Summary of the NMR restraints used for calculating the structures of LH1 α and β-polypeptides. Filled circles indicate strong hydrogen-bonding of the amide protons with their half-lives longer than 48 hours, and open circles indicate moderately strong hydrogen-bonding with half-lives longer than 12 hours but shorter than 48 hours. Sequential NOEs are presented as continuous lines extending over the peptide segment, and inter-residue NOEs are shown by lines connecting the starting and the ending residues.

from a series of H–^{2}H exchange experiments measured in $C^2HCl_3/C^2H_3O^2H$ (1:1). Of these, 31 and 26 consecutive backbone amide protons in the α and β-polypeptides were evaluated as being strongly hydrogen-bonded with their half-lives longer than 48 hours, indicating that the two polypeptides form highly stable secondary structures over the central domains. The amide signals from Leu14 to Glu36 of α-polypeptide and those from Glu13 to Ala37 of β-polypeptide can still be observed from the 2D ^{1}H–^{15}N HSQC spectra within a half-hour acquisition time after ten days of exchange. Notably, additional hydrogen bondings were observed in the α-polypeptide for the residues from Arg3 to Phe8, implying that a short helical structure is present in the N-terminal region. The hydrogen bonding information was included as additional distance restraints in the structure calculation. $^3J(H^N, H^\alpha)$ coupling constants measured with HNHA experiments fell in a range of 3∼6 Hz for most of the residues in the central portions of the two polypeptides, and somewhat greater values were revealed for the residues at terminal ends. The result suggests that the LH1 α and β-polypeptides of *R. rubrum* are largely α-helical over the central hydrophobic regions, consistent with the result of hydrogen bonding. Using the NOE derived distance constraints, the hydrogen bonding constraints and constraints for torsion angles (ϕ) derived from the $^3J(H^N, H^\alpha)$, the structures of α and β-polypeptides were calculated and energy minimized.

Description of the NMR solution structures

The NMR solution structures of LH1 α and β-polypeptides are shown in Figure 5. The stereo-views of ensembles were obtained by superimposing the backbone coordinates of the ten lowest energy structures from Asp9 to Gly43 of α-polypeptide and from Gly10 to Leu39 of β-polypeptide. Both the α and β-polypeptides revealed well-defined α-helical structures in the central hydrophobic regions. The backbone root-mean-square (r.m.s.) deviations over the 26 residues (Gln12-Arg37) of α-polypeptide and the 27 residues (Glu13-Leu39) of β-polypeptide were 0.86 Å and 0.89 Å (Table 1), respectively. The long helix was only slightly curved for the α-polypeptide and was almost straight for the β-polypeptide. Ribbon representations were used to show the positions of histidine residues that are considered to coordinate to the Mg of BChl *a* molecules. As expected from amino acid sequences, the His29 of α-polypeptide is

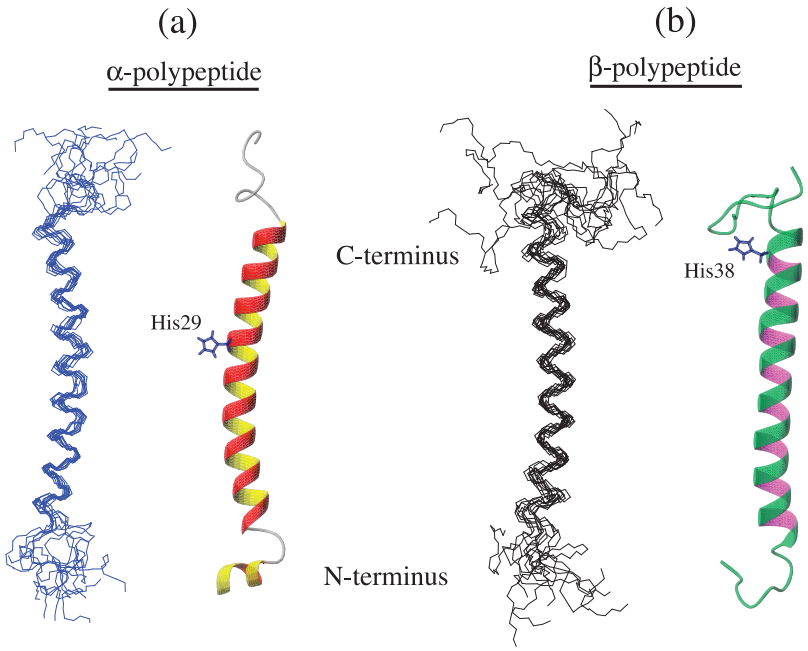

Figure 5. Solution structures of the (a) LH1 α-polypeptide and (b) β-polypeptide in C^2HCl_3/C^2H_3OH (1:1, v/v). Stereoviews (left side) represent the ten lowest energy conformers obtained by superimposing the backbone atoms of residues Asp9–Gly43 of α-polypeptide and residues Gly10–Leu39 of β-polypeptide, respectively. Ribbon representations (right side) show the positions of pigment-binding histidine residues. All images were produced using MOLMOL.[70]

located near the middle of the long helical region, while the His38 of β-polypeptide is at a position closed to the C-terminal end of the helix. Due to the absence of BChl *a*, side-chain conformation of the histidine residues appeared to be poorly defined, indicating that without pigment-binding the imidazole group is mobile in the solution. The N-terminal hydrophilic domain of β-polypeptide (Ala1–Ser7) and the C-terminal domains of α-polypeptide (Ser45–Ser52) and β-polypeptide (Trp42–Ser55) are unstructured. As predicted from the hydrogen bonding result, a short helical segment was identified in the N-terminal domain (Trp2–Gln6) of the α-polypeptide, followed by a three-residue unstructured loop (Leu7–Asp9). Quantitative evaluations of the calculated structures are summarized in Table 1.

The overall structures of the LH1 α and β-polypeptides from *R. rubrum* are different from the solution structures of LH1 β-polypeptide from *Rb. sphaeroides*,[29,30] but are very similar to the structures of the corresponding polypeptides of LH2 determined by X-ray crystallography from *Rps. acidophila*[3] and *Phaeospirillum* (formerly

Table 1. Structural statistics for the LH1 α and β-polypeptides

	α-Polypeptide	β-Polypeptide
NOE distance constraints	400	456
Intraresidue	151	163
Sequential	145	155
Medium-range ($i-j$=2, 3, 4)	104	136
Long-range ($i-j>4$)	0	2
Hydrogen bonds	36	39
Angle constraints (ϕ)	46	32
NOE constraint violations		
Largest (Å)	0.52	0.43
r.m.s. deviation (Å)	0.08	0.08
r.m.s. deviation from the mean structure (Å)		
All residues		
Backbone atoms	3.82±0.71	4.43±1.14
All heavy atoms	5.07±0.91	5.67±1.18
Residues in α-helices[a]		
Backbone atoms	0.86±0.27	0.89±0.35
All heavy atoms	1.64±0.31	1.66±0.34
Ramachandran plots		
Residues in allowed region (%)	95.9	95.3
Residues in disallowed region (%)	4.1	4.7
r.m.s. deviation from ideal geometry		
Bond lengths (Å)	0.0018±0.0002	0.0018±0.0003
Bond angles (deg.)	0.381±0.026	0.375±0.015
Improper (deg.)	0.194±0.018	0.189±0.022

[a] Residues for calculating the r.m.s. deviations are Gln12–Arg37 of α-polypeptide and Glu13–Leu39 of β-polypeptide, respectively.

Rhodospirillum) *molischianum*.[4] Because the structural subunits of *R. rubrum* LH1 and *Ps. molischianum* LH2 complexes share great similarities in amino acid sequence, spectral properties and reconstitution behavior,[31–33] the structures of LH2 polypeptides of *Ps. molischianum* were used as references for analyzing the structural features. Figure 6 shows comparisons of the structures of LH1 α and β-polypeptides with those of LH2 α and β-polypeptides from *Ps. molischianum* (PDB entry 1LGH). The central helical domain of the LH1 α-polypeptide can be well superimposed with that of the LH2 α-polypeptide over a range of about 25 residues (Figure 6(a)). The LH1 β-polypeptide gives an even more extensive fit to the LH2 β-polypeptide over the central region (Figure 6(b)). The short helix at the N terminus of LH1 α-polypeptide also shows a structural similarity to the corresponding portion of the LH2 α-polypeptide. Because the LH2 α-polypeptide is five residues longer at the N terminus if the histidine residues of the two polypeptides (His29 of LH1α and His34 of LH2α) are aligned at the same position of sequence, the N-terminal domains of the two structures can be compared by superimposing the backbone atoms around the flexible loops (Figure 6(c) and (d)). The result revealed that the N-terminal helices, the loops and the first eight residues of the central helices overlapped well with each other between the LH1 and LH2 α-polypeptides. The helix-loop-helix motif may be responsible for specific interactions with β-polypeptide in the N-terminal region to stabilize the structures of subunit and LH1 complexes (see below).

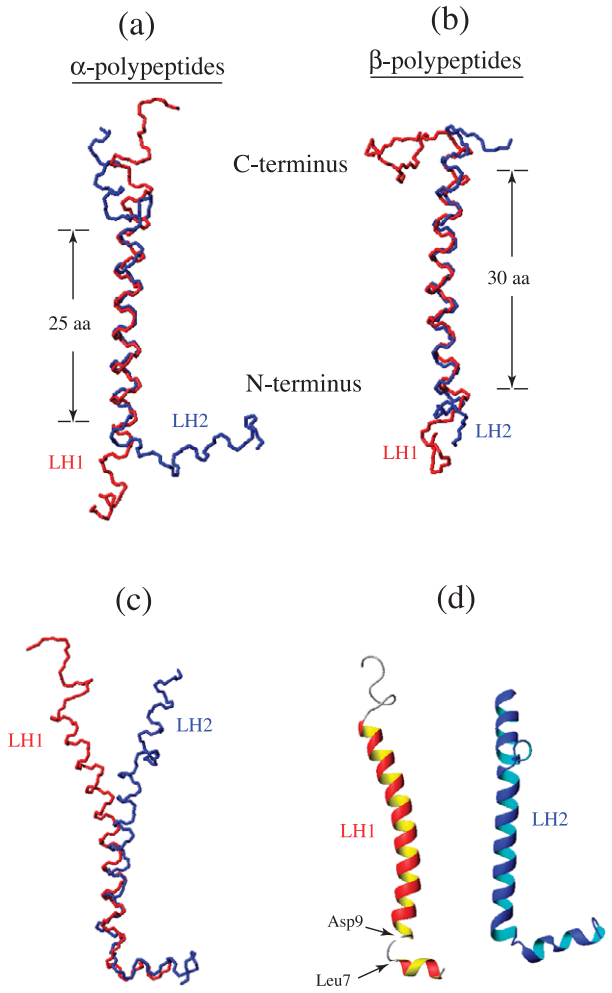

Figure 6. Comparison of the NMR solution structures of the *R. rubrum* LH1 polypeptides with X-ray crystal structures of the *Ps. molischianum* LH2 polypeptides. (a) Backbone superimposition over the central helical domains for the LH1 (red) and LH2 (blue) α-polypeptides. (b) Backbone superimposition over the central helical domains for the LH1 (red) and LH2 (blue) β-polypeptides. (c) Backbone superimposition of the N-terminal portion containing the short helices and loops of the LH1 (red) and LH2 (blue) α-polypeptides. (d) Ribbon representations showing the similarity of the N-terminal helices and loops between the LH1 and LH2 α-polypeptides.

Discussion

Although our NMR experiments were conducted using the samples dissolved in an organic solvent mixture, the structures obtained are considered to reflect the native folds of the LH1 α and β-polypeptides from *R. rubrum*. Previous studies showed that the LH1 β-polypeptide of *Rb. sphaeroides* had essentially the same structure in both the organic and detergent solutions.[28–30] Similar results have been reported for other membrane proteins including subunit c of the ATPase [34–36] and magainin antibiotic peptides.[37] An NMR solution structure of a larger membrane protein, the transmembrane domain of *E. coli* outer membrane protein A (19 kDa), has been demonstrated to be very similar to the crystal structure determined by X-ray diffraction.[38] The general folds of the LH1 α and β-polypeptides of this study are consistent with those observed from electron cryomicroscopy and X-ray crystallography for the RC–LH1 complexes. The projection maps at 8.5 Å obtained from two-dimensional RC–LH1 crystals indicate that the LH1 α and β-polypeptides of *R. rubrum* contain a substantial portion of their structure as transmembrane helices.[5,6,8] An electron density map at 4.8 Å resolution from the RC–LH1 crystals of *Rps. palustris* clearly shows that the transmembrane domains of the LH1 α and β-polypeptides are almost straight and can be well fitted by extended, helical structures.[11] The membrane-spanning regions of the NMR structures determined here also show a single helical fold for both of the *R. rubrum* LH1 α and β-polypeptides. However, the result is different from those reported for the LH1 β-polypeptide of *Rb. sphaeroides*, whose solution structures were shown to have a bent conformation consisting of two helices and a short, flexible loop located in almost the middle of the polypeptide.[28–30] The reason for the structural difference is not clear. Although genetically modified bacterial strains were used in the structural

determinations of the LH1 β-polypeptide from *Rb. sphaeroides*,[28–30] it seems unlikely that the genetic manipulations would affect the structure of the LH1 β-polypeptide (C. N. Hunter, personal communication). One possible reason is that different photosynthetic bacteria may have different structural organizations of light-harvesting complexes. The samples of this work were extracted from the wild-type strain of *R. rubrum*, which was grown under photosynthetic condition, and were purified as whole LH1 complex form before separation into the α and β-polypeptides by HPLC. The overall helix contents calculated from the solution structures were 73% and 60% for the α and β-polypeptides, respectively. These values are in good agreement with those measured from the CD spectra (Figure 1) and those previously reported with detergent solutions.[30,39]

With the structures of LH1 α and β-polypeptides available, we are able to construct a structural model for the B820 subunit. Figure 7 illustrates such a structure comprising the pigment molecules and polypeptides. The pigments were aligned on the basis of our previous NMR result,[27] in which the two BChl *a* adopt a non-equivalent, face-to-face configuration with partial overlap over the pyrrolic rings II, III and V. This pigment conformation in the B820 was confirmed recently by using chemically modified polypeptides.[33] On the analogy of the LH2 crystal structures,[3,4] there is no contact between the α and β-polypeptides in the transmembrane helical region where the interactions are mediated *via* the pigment molecules or buried water molecules. The only direct interaction between the two polypeptides is at the N and C-terminal ends. In the LH2 α-polypeptide, a 3_{10}-like helix comprising eight or 11 residues was found in the N-terminal domain, which was presumed to lie on the membrane surface and to involve interaction with the N-terminal residues of the β-apopolypeptide. Similarly, a short α-helical segment (Trp2-Gln6) is also present at N-terminal end of the *R. rubrum* LH1 α-polypeptide, followed by a three-residue loop and the membrane-spanning helix (Figure 6(c) and (d)). The N-terminal helix-loop-helix motif is for the first time identified in the LH1 α-polypeptide and is expected to play an important role in stabilizing the B820 subunit structure. Recent studies by Arluison *et al.*[25] and Parkes-Loach *et al.*[33] suggest that the first three N-terminal amino acid residues of the *R. rubrum* LH1 α-polypeptide form a cluster that is involved in hydrophobic interaction with the N-terminal extension of the β-polypeptide, contributing significantly to stabilizing the complex. Removal of these residues resulted in a decrease in association constant for the B820 and nearly eliminated the ability to form the LH1 complex.[33] The three residues in the α-polypeptide are shown here to form a part of the N-terminal helix. The short helical segment is presumed to point toward the β-polypeptide in the heterodimer (Figure 7) and is very likely to interact with the Gly10-Ile11-Thr12-Glu13-Gly14 sequence located at the N-terminal end of the transmembrane helix in the β-polypeptide as indicated in Figure 8.

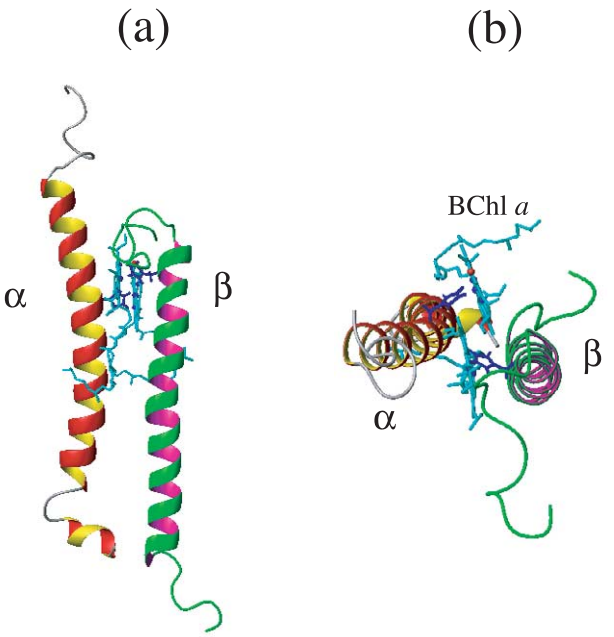

Figure 7. A model for the B820 subunit constructed using the LH1 α and β structures of this study and BChl *a* molecules. The structure of BChl *a* was adopted from the crystal structure of LH2 complex (PDB entry 1LGH) determined for *Ps. molischianum*. (a) Side view showing the BChl *a* alignment in the transmembrane helical domains and relative position of the N-terminal helix and loop of the α-polypeptide to the helical region of the β-polypeptide. (b) Top view of the structure in (a) from the C terminus showing the partial overlap between the two BChl *a* molecules colored in cyan.

It has become clear that the GxxxG motif, where two glycine residues are separated by any three amino acid residues on a helical framework, occurs frequently in the transmembrane domain of integral membrane proteins and acts as a universal scaffold for the transmembrane helix–helix association.[40–43] This arrangement of glycine residues gives rise to a flat surface on one face of the helix and permits the close approach of interacting helices. The GxxxG motif was first discovered in the transmembrane domain of glycophorin A and was determined as the key structural element responsible for its dimer formations. In this dimer, the interaction surface is composed of two ridges and their associated groove. One of the ridges formed by amino acid residues with large side-chains packs into the groove created by glycine in the opposite monomer.[44] It is highly likely that the GITEG segment in the LH1 β-polypeptide of *R. rubrum* also forms a structural motif that interacts with the N-terminal end of the LH1 α-polypeptide. The N-terminal amino acid residues with large side-chains (Trp2, Arg3, Trp4) in the α-polypeptide could act as ridges, allowing hydrophobic interaction with the groove formed by the GITEG motif in the β-polypeptide (Figure 8). The importance of the GITEG motif has

Figure 8. Schematic illustration of the primary and secondary structures of *R. rubrum* LH1 α and β-polypeptides. The two sequences and structures are aligned relative to the BChl *a*-liganding histidine residue. The short helical segment in the N terminus of α-polypeptide is shown to be located close to the GITEG sequence of the β-polypeptide. Illustrations of the secondary structures were produced using PROCHECK-NMR[69] and the shading indicates degree of accessibility to the solvent.

been demonstrated by a number of reconstitution experiments using truncated LH1 polypeptides.[21,24,25,45] Removal of the first four amino acid residues from the N terminus of LH1 β-polypolypeptide of *R. rubrum* has been shown to result in the formation of a B820 subunit and an LH1 complex with the native LH1 α-polypeptide, which are spectrally indistinguishable from those using the native LH1 β-polypeptide.[21] However, when the 17 or 18 amino acid residues were removed from the N terminus of *R. rubrum* LH1 β-polypeptide, in which the GITEG sequence is included, the truncated β-polypeptide failed to recognize the native LH1 α-polypeptide and tended to form a ββ-type homodimer with BChl *a*.[24,25,45] These results lead to a conclusion that a stretch of 9–13 amino acid residues at the N-terminal end of the LH1 α and β-polypeptide plays an important role in stabilizing the structure of the B820 heterodimer.[33] This is in good agreement with the conclusion derived from this study that the $G_{10}ITEG_{14}$ motif in the LH1 β-polypeptide of *R. rubrum* is involved in interactions with the N-terminal helix and loop of the LH1 α-polypeptide. Existence of the GxxxG motif in the β-polypeptide and its function for a helix–helix association may also provide an explanation for a previous observation[19] that the β-polypeptides alone in detergent solution favor a self-associated form and tend to form large aggregates.

Inspection of amino acid sequences of the LH1 β-polypeptides from other purple bacteria[46] reveals that the glycine residue corresponding to Gly10 in *R. rubrum* is conserved in all bacteria and there is also a GxxxG motif (GLTEG) at the same position in the LH1 β-polypeptide of *Rps. marina*. The residue corresponding to Gly14 in *R. rubrum*, however, is either an Ala for *Rps. acidophila*, or a Glu for *Rb. sphaeroides*, *Rb. capsulatus*, *Rps. viridis*, *Ectothiorhodospira halophila* and *Chromatium vinosum*. The GxxxA pattern is known as an alternative of the GxxxG motif and works in a similar way for mediating the helix–helix interactions in both membrane and soluble proteins.[47,48] The substitution of Glu for Gly or Ala, on the other hand, implies that in addition to the hydrophobic interaction electrostatic interaction may also contribute to stabilization of the subunit structure, since the negatively charged Glu in β-polypeptides is in close proximity to the positively charged residue (Arg or Lys) at the N-terminal ends of the α-polypeptides, which is present in all purple bacteria. Exchange of these charged N-terminal residues in the LH1 polypeptides by mutagenesis was shown to result in strong inhibition *in vivo* for the LH1 complex formation.[49,50]

In conclusion, the solution structures of the LH1 α and β-polypeptides from wild-type the purple photosynthetic bacterium *R. rubrum* have been determined using multidimensional NMR spectroscopy. Both the α and β-polypeptides exhibit a long α helix, comprising 32 amino acid residues, over the central membrane-spanning domain. The pigment-coordinating histidine residue (His29) in the α-polypeptide is located near the middle of the helix, while the corresponding histidine residue (His38) in the β-polypeptide is located close to the C-terminal end of the helix. A short helical segment (Trp2-Gln6) has been identified at the N terminus of the α-polypeptide, which is followed by a three-residue loop and the central transmembrane helix. The overall structures of the *R. rubrum* LH1 α and β-polypeptides are different from those previously reported for the LH1 β-polypeptide of *Rb. sphaeroides*, but are very similar to the structures of the corresponding LH2 α and β-polypeptides determined by X-ray crystallography. A structural model constructed for the B820 subunit using the solution structures reveals several important features of the interactions between the *R. rubrum* LH1 α and β-polypeptides. The significance of the N-terminal regions of the two polypeptides for stabilizing both B820 and LH1 complexes, as clarified by many experiments, can be attributed to the interactions between the short N-terminal helix (Trp2-Gln6) in the α-polypeptide and the GITEG motif in the β-polypeptide.

Materials and Methods

Preparation of the ^{13}C and ^{15}N-labeled LH1 α and β-polypeptides

Uniformly ^{15}N labeled α and β-polypeptides were prepared by growing the *R. rubrum* cells in a medium (pH 6.8) containing 1.0 g/l of $^{15}NH_4Cl$ ($^{15}N > 98\%$) and 6.0 g/l of DL-malic acid as the sole nitrogen and carbon sources, respectively.[51] To obtain ^{13}C and ^{15}N doubly labeled samples, the DL-malic acid in the above medium was replaced by $^{13}CH_3{}^{13}COONa$ ($^{13}C > 99\%$) at a

concentration of 0.8 g/l. The cells were grown under light conditions at 30 °C for two and four weeks for the ^{15}N and $^{15}N/^{13}C$ media, respectively. Isolation and purification of the LH1 complex were conducted as described elsewhere.[19,27] Chromatophores were prepared by sonication of the whole cells suspended in 50 mM phosphate buffer (pH 7.0) followed by differential centrifugation. The LH1 complex was extracted from the chromatophores by 0.35% (w/v) lauryldimethylamine *N*-oxide (LDAO) and purified by a DEAE column (25 mm×250 mm, Toyopearl 650S, TOSOH). The purified LH1 complex was first treated with benzene and then methanol to remove carotenoid and BChl *a*. The α and β-polypeptides were separated from the apopolypeptides by HPLC on a reverse-phase column (TSKgel, ODS-80Ts, 21.5 mm× 300 mm, TOSOH) using a linear gradient.[13]

CD measurements

CD spectra were recorded on a Jasco J-720w spectropolarimeter with a cuvette of 1 cm path-length. The wavelength range was set from 300 nm to 200 nm. The scan speed was 20 nm/minute, the band width 1.0 nm and the response 1 s. The apopolypeptides were dissolved in organic solvents of acetonitrile/2-propanol (2:1, v/v) containing 0.1%, v/v trifluoroacetic acid. Molar extinction coefficients used for determining the polypeptide concentrations were $\varepsilon_{280}=17{,}400\ M^{-1}\ cm^{-1}$ and $18{,}790\ M^{-1}\ cm^{-1}$ for the α and β-polypeptides, respectively, as calculated from their amino acid compositions. These values were also confirmed by our experiment in which the absorbances at 280 nm were measured for several HPLC-purified apoproteins of precisely weighed amounts in 2:1, v/v acetonitrile/2-propanol solutions containing 0.1% TFA. The CD spectra were corrected for background and converted to mean residue molar ellipticity. The helix contents were estimated from $[\theta]_{222}$ values.[52]

NMR spectroscopy

All NMR experiments were performed on a Bruker AVANCE DRX-400 spectrometer at 25 °C. A 5 mm TXI triple-resonance inverse probe with *z*-axis field gradient was used. The α-polypeptide was directly dissolved in C^2HCl_3/C^2H_3OH(1:1, v/v), whereas the β-polypeptide was first treated with trifluoroacetic acid and then dissolved in C^2HCl_3/C^2H_3OH (1:1, v/v). The final concentrations of both polypeptides were approximately 1 mM. Two-dimensional ^1H–^{15}N HSQC spectra were acquired with the pulse sequence of phase-sensitive echo/antiecho-TPPI gradient selection[53] using the ^{15}N-labeled samples. The sequential backbone assignments of ^1H, ^{13}C and ^{15}N resonances were made using standard three-dimensional triple-resonance HNCO,[54] HNCA,[55] HN(CO)CA,[56] CBCANH,[57] CBCA(CO)NH,[58] HBHANH,[59] and HBHA(CO)NH[60] experiments. Side-chain resonances were assigned from three-dimensional ^{15}N TOCSY-HSQC,[53] H(CC)(CO)NH[61,62] and HCCH-TOCSY[63] data. The NOE-derived distance restraints were obtained from three-dimensional ^{15}N NOESY-HSQC[53] spectra with a mixing time of 200 ms. The $^3J(H^N, H^\alpha)$ coupling constants were measured from a three-dimensional HNHA spectrum[64] and were used to determine ϕ-angle restraints. Slow-exchanging amide protons were identified from a series of two-dimensional ^1H–^{15}N HSQC spectra recorded after dissolving of the lyophilized α and β-polypeptides in $C^2HCl_3/C^2H_3O^2H$ (1:1, v/v). Strength of the hydrogen bonding was evaluated from the peak volume. Amide protons with a half-life longer than 12 hours were classified as being hydrogen-bonded and those with a half-life longer than 48 hours were classified as being strongly hydrogen-bonded. ^1H and ^{13}C chemical shifts were referenced directly to tetramethyl silane at 0 ppm, and ^{15}N were referenced indirectly.[65] NMR spectra were processed with NMRPipe[66] and analyzed using NMRView.[67]

Structure calculations

Structures of the α and β-apopolypeptides were calculated by a distance geometry simulated annealing protocol using CNS.[68] Distance restraints were obtained by converting NOE peak intensities into distance upper limits with d(strong)=3.0 Å, d(medium)=4.5 Å and d(weak)=5.5 Å. Each hydrogen bond was represented by two distance restraints (N–O 2.4–3.0 Å and H^N–O 1.9–2.3 Å) for maintaining linear bond geometry. A total of 300 random structures were calculated and subjected to one cycle of 3000 steps of heating at 6000 K and 3000 steps of annealing followed by 1000 steps of conjugate gradient energy minimization. The ten lowest energy structures for each polypeptide were selected to represent the three-dimensional folds. Structural quality was analyzed using AQUA and PROCHECH-NMR.[69] Graphical images were prepared with MOLMOL.[70]

Data Bank accession numbers

Coordinates have been deposited in the RCSB Protein Data Bank (entry 1XRD and 1WRG). Assignments of the α and β-polypeptides have been deposited at the BMRB (accession numbers: 6349 for α and 6350 for β).

Acknowledgements

This work was supported by Grants-in-aid for Scientific Research (nos 12878108 and 14550784), and for Scientific Research on Priority Areas "Structures of Biological Macromolecular Assemblies". This work has been partially supported by the Collaborative Research in Center for Interdisciplinary Research, Tohoku University, and by a grant from Takeda Science Foundation, Japan.

References

1. Deisenhofer, J., Epp, O., Miki, K., Huber, R. & Michel, H. (1985). Structure of the protein subunits in the photosynthetic reaction centre of *Rhodopseudomonas viridis* at 3 Å resolution. *Nature*, **318**, 618–624.
2. Allen, J. P., Feher, G., Yeates, T. O., Komiya, H. & Rees, D. C. (1987). Structure of the reaction center from *Rhodobacter sphaeroides* R-26: the cofactors. *Proc. Natl Acad. Sci. USA*, **84**, 5730–5734.
3. McDermott, G., Prince, D. M., Freer, A. A., Hawthornthwaite-Lawless, A. M., Papiz, M. Z., Cogdell, R. J. & Isaac, N. W. (1995). Crystal structure of an integral membrane light-harvesting complex from photosynthetic bacteria. *Nature*, **374**, 517–521.
4. Koepke, J., Hu, X., Muenke, C., Schulten, K. & Michel,

H. (1996). The crystal structure of the light-harvesting complex II (B800-B850) from *Rhodospirillum molischianum*. *Structure*, **4**, 581–597.
5. Karrasch, S., Bullough, P. A. & Ghosh, R. (1995). The 8.5 Å projection map of the light-harvesting complex I from *Rhodospirillum rubrum* reveals a ring composed of 16 subunits. *EMBO J.* **14**, 631–638.
6. Jamieson, S. J., Wang, P., Qian, P., Kirkland, J. Y., Conroy, M. J., Hunter, C. N. & Bullough, P. A. (2002). Projection structure of the photosynthetic reaction centre-antenna complex of *Rhodospirillum rubrum* at 8.5 Å resolution. *EMBO J.* **21**, 3927–3935.
7. Scheuring, S., Seguin, J., Marco, S., Levy, D., Robert, B. & Rigaud, J.-L. (2003). Nanodissection and high-resolution imaging of the *Rhodopseudomonas viridis* photosynthetic core complex in native membranes by AFM. *Proc. Natl Acad. Sci. USA*, **100**, 1690–1693.
8. Fotiadis, D., Qian, P., Philippsen, A., Bullough, P. A., Engel, A. & Hunter, C. N. (2004). Structural analysis of the reaction center light-harvesting complex I photosynthetic core complex of *Rhodospirillum rubrum* using atomic force microscopy. *J. Biol. Chem.* **279**, 2063–2068.
9. Jungas, C., Ranck, J.-L., Rigaud, J.-L., Joliot, P. & Vermeglio, A. (1999). Supramolecular organization of the photosynthetic apparatus of *Rhodobacter sphaeroides*. *EMBO J.* **18**, 534–542.
10. Scheuring, S., Francia, F., Busselez, J., Melandris, B. A., Rigaud, J.-L. & Levy, D. (2004). Structural role of PufX in the dimerization of the photosynthetic core complex of *Rhodobacter sphaeroides*. *J. Biol. Chem.* **279**, 3620–3626.
11. Roszak, A. W., Howard, T. D., Southall, J., Gardiner, A. T., Law, C. J., Isaac, N. W. & Cogdell, R. J. (2003). Crystal structure of the RC–LH1 core complex from *Rhodopseudomonas palustris*. *Science*, **302**, 1969–1972.
12. Miller, J. F., Hinchigeri, S. B., Parkes-Loach, P. S., Callahan, P. M., Sprinkle, J. R., Riccobono, J. R. & Loach, P. A. (1987). Isolation and characterization of a subunit form of the light-harvesting complex of *Rhodospirillum rubrum*. *Biochemistry*, **26**, 5055–5062.
13. Parkes-Loach, P. S., Sprinkle, J. R. & Loach, P. A. (1988). Reconstitution of the B873 light-harvesting complex of *Rhodospirillum rubrum* from the separately isolated α- and β-polypeptides and bacteriochlorophyll *a*. *Biochemistry*, **27**, 2718–2727.
14. Chang, M. C., Callahan, P. M., Parkes-Loach, P. S., Cotton, T. M. & Loach, P. A. (1990). Spectroscopic characterization of the light-harvesting complex of *Rhodospirillum rubrum* and its structural subunit. *Biochemistry*, **29**, 421–429.
15. Visschers, R. W., Chang, M. C., van Mourik, F., Parkes-Loach, P. S., Heller, B. A., Loach, P. A. & van Grondelle, R. (1991). Fluorescence polarization and low-temperature absorption spectroscopy of a subunit form of light-harvesting complex I from purple photosynthetic bacteria. *Biochemistry*, **30**, 5734–5742.
16. van Mourik, F., van der Oord, C. J. R., Visscher, K. J., Parkes-Loach, P. S., Parkes, P. A., Visschers, R. W. & van Grondelle, R. (1991). Exciton interactions in the light-harvesting antenna of photosynthetic bacteria studied with triplet–singlet spectroscopy and singlet–triplet annihilation on the B820 subunit form of *Rhodospirillum rubrum*. *Biochim. Biophys. Acta*, **1059**, 111–119.
17. Visschers, R. W., van Grondelle, R. & Robert, B. (1993). Resonance Raman spectroscopy of the B820 subunit of the core antenna from *Rhodospirillum rubrum* G9. *Biochim. Biophys. Acta*, **1183**, 369–373.
18. Pandit, A., Visschers, R. W., van Stokkum, I. H. M., Kraayenhof, R. & van Grondelle, R. (2001). Oligomerization of light-harvesting I antenna peptides of *Rhodospirillum rubrum*. *Biochemistry*, **40**, 12913–12924.
19. Wang, Z.-Y., Muraoka, Y., Nagao, M., Shibayama, M., Kobayashi, M. & Nozawa, T. (2003). Determination of the B820 subunit size of a bacterial core light-harvesting complex by small-angle neutron scattering. *Biochemistry*, **42**, 11555–11560.
20. Loach, P. A., Parkes-Loach, P. S., Davis, C. M. & Heller, B. A. (1994). Probing protein structural requirements for formation of the core light-harvesting complex of photosynthetic bacteria using hybrid reconstitution methodology. *Photosynth. Res.* **40**, 231–245.
21. Meadows, K. A., Iida, K., Tsuda, K., Recchia, P. A., Heller, B. A., Antonio, B. *et al*. (1995). Enzymatic and chemical cleavage of the core light-harvesting polypeptides of photosynthetic bacteria: determination of the minimal polypeptide size and structure required for subunit and light-harvesting complex formation. *Biochemistry*, **34**, 1559–1574.
22. Davis, C. M., Parkes-Loach, P. S., Cook, C. K., Meadows, K. A., Bandilla, M., Scheer, H. & Loach, P. A. (1996). Comparison of the structural requirements for bacteriochlorophyll binding in the core light-harvesting complexes of *Rhodospirillum rubrum* and *Rhodobacter sphaeroides* using reconstitution methodology with bacteriochlorophyll analogs. *Biochemistry*, **35**, 3072–3084.
23. Davis, C. M., Bustamante, P. L., Todd, J. B., Parkes-Loach, P. S., McGlynn, P., Olsen, J. D., McMaster, L. *et al*. (1997). Evaluation of structure–function relationships in the core light-harvesting complex of photosynthetic bacteria by reconstitution with mutant polypeptides. *Biochemistry*, **36**, 3671–3679.
24. Meadows, K. A., Parkes-Loach, P. S., Kehoe, J. W. & Loach, P. A. (1998). Reconstitution of core light-harvesting complexes of photosynthetic bacteria using chemically synthesized polypeptides. 1. Minimal requirements for subunit formation. *Biochemistry*, **38**, 3411–3417.
25. Arluison, V., Seguin, J., Le Caer, J.-P., Sturgis, J. N. & Robert, B. (2004). Hydrophobic pockets at the membrane interface: an original mechanism for membrane protein interactions. *Biochemistry*, **43**, 1276–1282.
26. Sturgis, J. N., Olsen, J. D., Robert, B. & Hunter, C. N. (1997). Functions of conserved tryptophan residues of the core light-harvesting complex of *Rhodobacter sphaeroides*. *Biochemistry*, **36**, 2772–2778.
27. Wang, Z.-Y., Muraoka, Y., Shimonaga, M., Kobayashi, M. & Nozawa, T. (2002). Selective detection and assignment of the solution NMR signals of bacteriochlorophyll *a* in a reconstituted subunit of a light-harvesting complex. *J. Am. Chem. Soc.* **124**, 1072–1078.
28. Kikuchi, J., Asakura, T., Loach, P. A., Parkes-Loach, P. S., Shimada, K., Hunter, C. N. *et al*. (1999). A light-harvesting antenna protein retains its folded conformation in the absence of protein–lipid and protein–pigment interactions. *Biopolymers*, **49**, 361–372.
29. Conroy, M. J., Westerhuis, W. H. J., Parkes-Loach, P. S., Loach, P. A., Hunter, C. N. & Williamson, M. P. (2000). The solution structure of *Rhodobacter sphaeroides* LH1β reveals two helical domains separated by a more flexible region: structural consequences for the LH1 complex. *J. Mol. Biol.* **298**, 83–94.
30. Sorgen, P. L., Cahill, S. M., Krueger-Koplin, R. D., Krueger-Koplin, S. T., Schenck, C. C. & Girvin, M. E.

(2002). Structure of the *Rhodobacter sphaeroides* light-harvesting 1 β subunit in detergent micelles. *Biochemistry*, **41**, 31–41.
31. Germeroth, L., Lottspeich, F., Robert, B. & Michel, H. (1993). Unexpected similarities of the B800-850 light-harvesting complex from *Rhodospirillum molischianum* to the B870 light-harvesting complexes from other purple photosynthetic bacteria. *Biochemistry*, **32**, 5615–5621.
32. Todd, J. B., Parks-Loach, P. A., Leykam, J. F. & Loach, P. A. (1998). *In vitro* reconstitution of the core and peripheral light-harvesting complexes of *Rhodospirillum molischianum* from separately isolated components. *Biochemistry*, **37**, 17458–17468.
33. Parkes-Loach, P. S., Majeed, A. P., Law, C. J. & Loach, P. A. (2004). Interactions stabilizing the structure of the core light-harvesting complex (LH1) of photosynthetic bacteria and its subunit (B820). *Biochemistry*, **43**, 7003–7016.
34. Girvin, M. E., Rastogi, V. K., Abildgaard, F., Markley, J. L. & Fillingame, R. H. (1998). Solution structure of the transmembrane H^+-transporting subunit c of the F_1F_o ATP synthase. *Biochemistry*, **37**, 8817–8824.
35. Matthey, U., Kaim, G., Braun, D., Wuthrich, K. & Dimroth, P. (1999). NMR studies of subunit c of the ATP synthase from *Propionigenium modestum* in dodecylsulphate micelles. *Eur. J. Biochem.* **261**, 459–467.
36. Krueger-Koplin, R. D., Sorgen, P. L., Krueger-Koplin, S. T., Rivera-Torres, I. O., Cahill, S. M., Hicks, D. B. *et al*. (2004). An evaluation of detergents for NMR structural studies of membrane proteins. *J. Biomol. NMR*, **17**, 43–57.
37. Gesell, J., Zasloff, M. & Opella, S. J. (1997). Two-dimensional ^{1}H NMR experiments show that the 23-residue magainin antibiotic peptide is an α-helix in dodecylphosphocholine micelles, sodium dodecylsulfate micelles, and trifluoroethanol/water solution. *J. Biomol. NMR*, **9**, 127–135.
38. Arora, A., Abildgaard, F., Bushweller, J. H. & Tamm, L. K. (2001). Structure of outer membrane protein A transmembrane domain by NMR spectroscopy. *Nature Struct. Biol.* **8**, 334–338.
39. Ghosh, R., Hauser, H. & Bachofen, R. (1988). Reversible dissociation of the B873 light-harvesting complex from *Rhodospirillum rubrum* G9+. *Biochemistry*, **27**, 1004–1014.
40. Russ, W. P. & Engelman, D. M. (2000). The GxxxG motif: a framework for transmembrane helix–helix association. *J. Mol. Biol.* **296**, 911–919.
41. Senes, A., Gerstein, M. & Engelman, D. M. (2000). Statistical analysis of amino acid patterns in transmembrane helices: the GxxxG motif occurs frequently and in association with β-branched residues at neighboring positions. *J. Mol. Biol.* **296**, 921–936.
42. Kleiger, G., Grothe, R., Mallick, P. & Eisenberg, D. (2002). GXXXG and AXXXA common α-helical interaction motifs in proteins, particularly in extremophiles. *Biochemistry*, **41**, 5990–5997.
43. Melnyk, R. A., Kim, S., Currant, A. R., Engelman, D. M., Bowie, J. U. & Deber, C. M. (2004). The affinity of GXXXG motifs in transmembrane helix–helix interactions is modulated by long-range communication. *J. Biol. Chem.* **279**, 16591–16597.
44. MacKenzie, K. R., Prestegard, J. H. & Engelman, D. M. (1997). A transmembrane helix dimer: structure and implications. *Science*, **276**, 131–133.
45. Kehoe, J. W., Meadows, K. A., Parkes-Loach, P. S. & Loach, P. A. (1998). Reconstitution of core light-harvesting complexes of photosynthetic bacteria using chemically synthesized polypeptides. 2. Determination of structural features that stabilize complex formation and their implications for the structure of the subunit complex. *Biochemistry*, **38**, 3418–3428.
46. Zuber, H. & Cogdell, R. J. (1995). Structure and organization of purple bacterial antenna complexes. In *Anoxygenic Photosynthetic Bacteria* (Blankenship, R. E., Madigan, M. T. & Bauer, C. D., eds), pp. 315–348, Kluwer Academic Publishers, Dordrecht, The Netherlands.
47. Kleiger, G. & Eisenberg, D. (2002). GXXXG and GXXXA motifs stabilize FAD and NAD(P)-binding Rossmann folds through C^{α}–H···O hydrogen bonds and van der Waals interactions. *J. Mol. Biol.* **323**, 69–76.
48. Kairys, V., Gilson, M. K. & Luy, B. (2004). Structural model for an AXXXG-mediated dimer of surfactant-associated protein C. *Eur. J. Biochem.* **271**, 2086–2092.
49. Dörge, B., Klug, G., Gad'on, N., Cohen, S. N. & Drews, G. (1990). Effects on the formation of antenna complex B870 of *Rhodobacter capsulatus* by exchange of charged amino acids in the N-terminal domains of the α and β pigment-binding proteins. *Biochemistry*, **29**, 7754–7758.
50. Stiehle, H., Cortez, N., Klug, G. & Drews, G. (1990). Negatively charged N terminus in the α polypeptide inhibits formation of light-harvesting complex I in *Rhodobacter capsulatus*. *J. Bacteriol.* **172**, 7131–7137.
51. Ormerod, J. G., Ormerod, K. S. & Gest, H. (1961). Light-dependent utilization of organic compounds and photoproduction of molecular hydrogen by photosynthetic bacteria; relationships with nitrogen metabolism. *Arch. Biochem. Biophys.* **94**, 449–463.
52. Chen, Y.-H., Yang, J. T. & Martinez, M. (1972). Determination of the secondary structures of proteins by circular dichroism and optical rotatory dispersion. *Biochemistry*, **11**, 4120–4131.
53. Davis, A. L., Keeler, J., Laue, E. D. & Moskau, D. (1992). Experiments for recording pure-absorption heteronuclear correlation spectra using pulsed field gradients. *J. Magn. Reson.* **98**, 207–216.
54. Kay, L. E., Xu, G.-Y. & Yamazaki, T. (1994). Enhanced-sensitivity triple-resonance spectroscopy with minimal H_2O saturation. *J. Magn. Reson. ser. A*, **109**, 129–133.
55. Stonehouse, J., Clowes, R. T., Shaw, G. L., Keeler, J. & Laue, E. D. (1995). Minimisation of sensitivity losses due to the use of gradient pulses in triple-resonance NMR of protein. *J. Biomol. NMR*, **5**, 226–232.
56. Bax, A. & Pochapsky, S. S. (1992). Optimized recording of heteronuclear multidimensional NMR spectra using pulsed field gradients. *J. Magn. Reson.* **99**, 638–643.
57. Grzesiek, S. & Bax, A. (1992). An efficient experiment for sequential backbone assignment of medium-sized isotopically enriched proteins. *J. Magn. Reson.* **99**, 201–207.
58. Muhandiram, D. R. & Kay, L. E. (1994). Gradient-enhanced triple-resonance three-dimensional NMR experiments with improved sensitivity. *J. Magn. Reson. ser. B*, **103**, 203–216.
59. Wang, A. C., Lodi, P. J., Qin, J., Vuister, G. W., Gronenborn, A. M. & Clore, G. M. (1994). An efficient triple-resonance experiment for proton-directed sequential backbone assignment of medium-sized proteins. *J. Magn. Reson. ser. B*, **105**, 196–198.
60. Grzesiek, S. & Bax, A. (1993). Amino acid type

determination in the sequential assignment procedure of uniformly $^{13}C/^{15}N$-enriched proteins. *J. Biomol. NMR*, **3**, 185–204.
61. Grzesiek, S., Anglister, J. & Bax, A. (1993). Correlation of backbone amide and aliphatic side-chain resonances in $^{13}C/^{15}N$-enriched proteins by isotropic mixing of ^{13}C magnetization. *J. Magn. Reson. ser. B*, **101**, 114–119.
62. Logan, T. M., Olejniczak, E. T., Xu, R. X. & Fesik, S. W. (1993). A general method for assigning NMR spectra of denatured proteins using 3D HC(CO)NH-TOCSY triple resonance experiments. *J. Biomol. NMR*, **3**, 225–231.
63. Kay, L. E., Xu, G.-Y., Singer, A. U., Muhandiram, D. R. & Forman-Kay, J. D. (1993). A gradient-enhanced HCCH-TOCSY experiment for recording side-chain ^{1}H and ^{13}C correlations in H_2O samples of proteins. *J. Magn. Reson. ser. B*, **101**, 333–337.
64. Vuister, G. W. & Bax, A. (1993). Quantitative J correlation: a new approach for measuring homonuclear three-bond $J(H^NH^\alpha)$ coupling constants in ^{15}N-enriched proteins. *J. Am. Chem. Soc.* **115**, 7772–7777.
65. Wishart, D. S., Bigam, C. G., Yao, J., Abildgaard, F., Dyson, H. J., Oldfield, E. *et al*. (1995). ^{1}H, ^{13}C and ^{15}N chemical shift referencing in biomolecular NMR. *J. Biomol. NMR*, **6**, 135–140.
66. Delaglio, F., Grzesiek, S., Zhu, G., Vuister, G. W., Pfeifer, J. & Bax, A. (1995). NMRPipe: a multidimensional spectral processing system based on UNIX pipes. *J. Biomol. NMR*, **6**, 277–293.
67. Johnson, B. A. & Blevins, R. A. (1994). NMRView: a computer program for the visualization and analysis of NMR data. *J. Biomol. NMR*, **4**, 603–614.
68. Brünger, A. T., Adams, P. D., Clore, G. M., DeLano, W. L., Gros, P., Grosse-Kunstleve, R. W. *et al*. (1998). Crystallography & NMR system: a new software suite for macromolecular structure determination. *Acta Crystallog. sect. D*, **54**, 905–921.
69. Laskowski, R. A., Rullmann, J. A. C., MacArthur, M. W., Kaptein, R. & Thornton, J. M. (1996). AQUA and ROCHECK-NMR: programs for checking the quality of protein structures solved by NMR. *J. Biomol. NMR*, **8**, 477–486.
70. Koradi, R., Billeter, M. & Wüthrich, K. (1996). MOLMOL: a program for display and analysis of macromolecular structures. *J. Mol. Graph.* **14**, 51–55.

Edited by M. F. Summers

(Received 20 October 2004; received in revised form 21 December 2004; accepted 4 January 2005)